**Boise State University**
**ScholarWorks**

Electrical and Computer Engineering Faculty Publications and Presentations

Department of Electrical and Computer Engineering

1-15-2011

# Electron Hop Funnel Measurements and Comparison with the Lorentz-2E Simulation

Charles Lester
*Boise State University*

Jim Browning
*Boise State University*

Lael Matthews
*Micron Technology*

© 2011 IEEE. Personal use of this material is permitted. Permission from IEEE must be obtained for all other uses, in any current or future media, including reprinting/republishing this material for advertising or promotional purposes, creating new collective works, for resale or redistribution to servers or lists, or reuse of any copyrighted component of this work in other works. DOI: 10.1109/TPS.2010.2087775

© 2011 IEEE. Personal use of this material is permitted. Permission from IEEE must be obtained for all other uses, in any current or future media, including reprinting/republishing this material for advertising or promotional purposes, creating new collective works, for resale or redistribution to servers or lists, or reuse of any copyrighted component of this work in other works. DOI: 10.1109/TPS.2010.2087775

# Electron Hop Funnel Measurements and Comparison with the Lorentz-2E Simulation

Charles Lester, *Student Member, IEEE,* Jim Browning, *Senior Member, IEEE,* and Lael Matthews

***Abstract*— Electron hop funnels have been fabricated using a Low Temperature Co-Fired Ceramic (LTCC). Measurements of the hop funnel I-V curve and electron energy distribution have been made using gated field emitters as the electron source. The charged particle simulation Lorentz 2E has been used to model the hop funnel charging and to predict the I-V and energy characteristics. The results of this comparison indicate that the simulation can be used to design hop funnel structures for use in various applications.**

***Index Terms*—electron emission, surface charging, vacuum microelectronics**

## I. Introduction

Field Emission Arrays (FEAs) have long been under development for use in a variety of devices including Field Emission Displays (FEDs) [1], [2] and Microwave Vacuum Electron Devices (MVEDs) [3]. One technique for improving the performance of FEAs is the use of a "hop funnel" [4] to concentrate the electron current density, improve beam uniformity, and protect the emitters from high electric fields and from ion or electron back bombardment. The theory behind hop funnel operation is described in detail in [4]. In a hop funnel structure, electrons are injected into an insulating funnel or slit. Electrons strike the insulating hop funnel wall, and secondary electrons [5]-[7] are generated. Charge builds up on the insulating wall with a dependence upon the incident electron energy and the secondary emission yield. An electrode (hop electrode) is placed at the top of the funnel to generate an electric field which pulls the electrons toward the funnel exit. If the electric field along the hop wall is large enough, all of the injected electron current will be extracted from the funnel resulting in unity gain [4]. Electrons "hop" along the wall surface and out of the structure. The use of hop funnels in FEDs has been demonstrated [8] to provide greatly improved uniformity. Measurements of the hop funnel I-V characteristics and beam energy spread [9], [10] have been made. These results have been compared with Monte Carlo based simulations.

Manuscript submitted May 21, 2010. This work was supported in part by the U.S. Air Force Office of Scientific Research under grant # FA9550-08-1-0396 and by the Electrical and Computer Engineering Department at Boise State University.

Charles Lester is with the Electrical and Computer Engineering Department at Boise State University, Boise, ID 83725 USA (e-mail: charleslester@u.boisestate.edu).

Jim Browning is with the Electrical and Computer Engineering Department at Boise State University, Boise, ID 83725 USA,( phone: 208-426-2347, e-mail: jimbrowning@boisestate.edu)

Lael Matthews is with the Micron Technology, Boise, ID 83716 USA

The application of such hop funnels can be improved with the use of electron optics design simulations which can be implemented into various devices: MVEDs, X-ray sources, FEDs. One such simulation is Integrated Engineering Software's (IES) Lorentz-2E particle trajectory code [11]. The simulation provides a platform for electron optics design, and we are attempting to benchmark the simulation against experimental results to see if the simulation is a useful tool for the design of devices using hop funnels. This paper represents the first in a series that will look at the mechanisms of the simulation, the stability of the simulation to setup parameters, and the ability of the simulation to model the experiment. In this paper, we look primarily at the simulation approach and the stability, and we compare the simulation predictions with basic experimental results.

Hop funnel devices have been fabricated and demonstrated using a variety of glass funnels shapes [4],[8]-[10]. The funnels have been fabricated by sandblasting and by etching. Our group has fabricated hop funnels by milling a funnel hole in Dupont 951 Green Tape™ Low Temperature Co-fired Ceramic (LTCC) [12]. Measurements of the hop funnel I-V characteristics and the energy distribution of extracted electrons have been performed using FEAs as the electron source.

## II. The Lorentz Simulation

### A. Simulation Description

The simulation used in this work is the Lorentz 2E two-dimensional model. The geometry setup is shown in Fig. 1., where the hop funnel, hop electrode, and electron source are indicated. The hop funnel has an entrance diameter of 2.3 mm, and exit diameter of 0.3 mm, and a thickness of 1.0 mm. The dielectric constant of 7.8 for LTCC is used for the funnel [12]. The geometry here is rotationally symmetric. In the simulation setup, the injected current is set to a fixed value for a given emission object. The emission current is dynamically represented as a number of charge rays that each maintains a constant mass to charge ratio equal to that of an electron [11]. The hop funnel wall is set as a secondary emitting object. The secondary emission characteristics are determined using a semi-empirical model [13], [14] with four function inputs: maximum secondary emission yield $\delta_e$, energy at the maximum yield $W_m$, average energy of the secondary electron $W_{avg}$, and the surface roughness (a value from 0 to 2 with 0 being smooth). When a secondary segment is defined, the segment can be broken down into smaller elements. The net charge deposited by the incoming and secondary emitted electrons is then calculated for each element of each segment.

© 2011 IEEE. Personal use of this material is permitted. Permission from IEEE must be obtained for all other uses, in any current or future media, including reprinting/republishing this material for advertising or promotional purposes, creating new collective works, for resale or redistribution to servers or lists, or reuse of any copyrighted component of this work in other works. DOI: 10.1109/TPS.2010.2087775

Other objects are defined to collect the electrons, such as the anode placed above the hop funnel. Once the objects and voltages are defined, the fields are calculated using a Boundary Element Method.

For the hop funnel work, IES modified the Lorentz simulation to calculate the net deposited charge and track the new generations of secondary electrons. Primary electrons are emitted as charge rays from a defined emitter object. For constant injected emission current, the amount of charge per ray is determined by the defined emission current. Other emission options are available in the model, but experimentally, the current is maintained at an approximately fixed value. The charged particles are tracked using an adaptive Runge-Kutta technique. The accuracy of the method must be kept high, and the minimum time step size must be kept small ($\leq 10^{-11}$ s) to ensure that hopping electrons can be accurately modeled over short hopping distances (<5 μm).

The funnel geometry is rotationally symmetric, so the calculations include the current distributed over a circular area mapped out by each segment. The axis of symmetry is used as a "reflector", so electrons transiting this line are reflected back, as shown in Fig. 2. This figure shows the simulation results for primary and secondary electrons for a case when unity gain occurs. The results are discussed in more detail later.

The simulation flow is described here. Charge rays (primaries) are launched and tracked starting from the emitter object. The charge rays can then strike the hop walls or in some cases may go directly out of the funnel exit. The charge rays are tracked until they strike a collector and are removed or until they strike a secondary emitting surface such as the hop wall. Once all primaries are emitted, secondary charge ray emissions from the hop wall are launched for each wall element based on the past incident charge rays. These secondary charge rays are then tracked until the charge rays either reach a collector or strike the hop wall again. This process is repeated with another generation of secondary charge rays until no new secondaries are generated. The simulation then calculates the surface charge on the hop wall and recalculates the new electric field within the structure. This process constitutes one surface charge time step iteration. In general, the simulation requires many surface charge iterations to converge to a steady state solution. Therefore, the surface charge time step size can be very important in allowing a stable build up of surface charge on the hop funnel wall. Once the new electric field is calculated, a new set of primary charge rays are again launched from the emitter, and the resulting secondary electrons are again followed. Furthermore, if the electric field is high enough, nearly all of the injected current will eventually make it out of the funnel and will be collected at the anode. Thus, for sufficiently high hop electrode voltage, the anode current will equal the injected current in the steady state regime. This is referred to as unity gain.

In general, the simulation will be initialized with an uncharged hop funnel surface, and the number of charge rays that exit the hop structure and get collected at the anode will vary as a function of the surface charge time step iteration. As the simulation continues, the hop funnel surface charge density and anode current will reach steady state if proper values for the simulation parameters are specified. The current output versus time is used here as the main diagnostic to analyze the simulation stability for various input parameters.

### *B. Simulation Stability*

Several parameters in the simulation setup that characterize the semi-empirical secondary electron emission process and other key parameters can significantly affect the simulation stability and the results.

The surface element size of the secondary emitter wall of the hop funnel must be chosen to be sufficiently small. Too few elements will create large charge build up on too few elements, and the problem will be poorly modeled. Another important aspect is the electron hop distance. If an electron hops a relatively short distance due either to a weak electric field or a very shallow wall slope, it is possible that a hopping electron will always end up back on the same element. Therefore, the elements size must be small enough that the average secondary electron will hop to a different element.

In addition, the number of rays is also important to make certain the charge is well distributed over the secondary emitting wall without slowing down the simulation too much. Too few rays will result in large amounts of charge being deposited on just a few elements.

Finally, if the surface charge time step size is too large, or the injected current is too large, the charge per ray will be large enough such that the surface charge density fluctuations on the secondary emitting wall will vary wildly, and the resulting anode current will fluctuate rapidly as well. If the steps are too small, then the run time will be very long. In particular, for a total injected charge ray number $N$, a surface charge time step $\Delta t$, and an injected current $I$, the charge per ray is $\Delta Q = I \cdot \Delta t / N$. $\Delta Q$ is the most basic quantity which determines how much charge is carried per ray and then deposited on the hop funnel surface per time step iteration.

A test case was used to analyze the stability of the simulation for the following fixed parameters. The surface element number was set to 100 (~14 μm). The total injected current was set to 1 μA. The hop electrode was set to 600 V, and the anode voltage was set to 800 V. These parameters were all chosen based on the experimental results which are discussed later. In addition, the empirical parameters for the secondary emission must also be set. These values are not known for LTCC, so starting values were chosen for the stability tests of $\delta_e$ = 3.0, $W_m$ = 420 eV, and $W_{avg}$ = 5 eV, which is similar to the secondary emission parameters of glass [15].

Using the parameters listed above, the test case consisted of nine runs as shown in Table 1. Each column represents three different runs with a total injected ray number and time step size chosen so that each column maintains a constant charge per ray value $\Delta Q = I \cdot \Delta t / N$. Thus, the rows of a given column of Table 1 will give the effects of increasing or decreasing how the charge is spatially distributed by increasing or decreasing the total injected ray number $N$, whereas comparing adjacent columns will yield information about the effects of increasing the charge per ray $\Delta Q$.

For the test case, the gated FEA was modeled by uniform emission from a straight line segment set to the equivalent

© 2011 IEEE. Personal use of this material is permitted. Permission from IEEE must be obtained for all other uses, in any current or future media, including reprinting/republishing this material for advertising or promotional purposes, creating new collective works, for resale or redistribution to servers or lists, or reuse of any copyrighted component of this work in other works. DOI: 10.1109/TPS.2010.2087775

field emitter gate voltage of 65 V. The charge rays were then injected with an initial kinetic energy of 65 eV from the segment rather than from individual gated emitter tips. This approach does not affect the stability results but does reduce computation time needed to model each field emitter gate-tip structure. However, for the actual experimental modeling (Section C), the field emitter model was modified for a more accurate representation. The injected primary current was 1 µA.

For the first two columns of table 1, the time step size is small enough that a larger time step sequence is initially needed to bring the surface charge close to the steady state value; otherwise the simulation will require too many time steps to be practical. Once the simulation is near steady state, the final step size (Those listed in the first two columns of Table 1) is run until steady state is achieved. The initial time step ramp is 5 µs for time steps 1– 69 and then 1 µs for time steps 70 – 99. These steps represent a simulation time equivalent of 380 µs. The anode current versus time during the ramp up period is shown in Fig. 3. As can be seen, the current out of the funnel begins very low and then increases as the simulation time increases. After the simulation equivalent of ~200 µs, the current levels approach steady state. However, the current fluctuation is still large. It is after this point that the stability of the simulation is compared for the different cases given in Table 1.

The results of the nine runs of Table 1 are shown in the steady state regime in Fig. 4 – 6. These graphs show the anode current versus time during the steady state part of the curve (after 350 µs). For each case the standard deviation of the anode current is calculated and is shown on the graph. Figures 4 and 5 demonstrate that the fluctuation of the anode current is approximately constant for constant charge per ray. In Fig. 6, the standard deviation changes from 5.6% to 10.2% for a decreasing total number of injected charge rays. The main result is that the current fluctuation decreases as the charge per ray is decreased. Fig. 6 shows that the anode current becomes unstable as the charge per ray approaches 300k electrons per ray with a standard deviation as high as 43.5%. The Fig. 6 cases give the largest standard deviations of all three columns of Table 1, and plots (a) and (b) are visually unstable, but plot (c) is surprisingly stable. From this result, a $\Delta t \leq 5$ µs step size with 200 rays appears to be adequate when used with the semi-empirical secondary electron emission parameters and injected current used in this test case.

The surface charge density is shown in Fig. 7 for the simulation case of Fig. 5(a). The surface charge is shown for the steady state condition. As can be seen, the hop funnel wall charges up negative. This negative charge decreases the kinetic energy of the electron upon impact with the wall such that the kinetic energy is approximately equal to the first crossover point (the first point at which $\delta(W) = 1$) of the secondary yield curve of the semi-empirical secondary emission model.

In general, for $W_m = 420$ eV, the value of the maximum yield of $\delta_e = 3.0$ causes many secondary electron generations, and small time step sizes are needed to achieve stability. Ultimately, the test cases serve as a basis for choosing the simulation parameters to achieve stability. However, the values for the semi-empirical secondary electron emission model that will be chosen to approximate LTCC will be based on the comparison of the energy and I-V characteristics of the simulation results against the measured hop funnel results.

### *C. Simulation of Experiment*

An example of a simulation run is shown in Fig. 2. Note that the electrons are emitted from discrete locations which represent field emitters. The electrons are also injected with an angular distribution. The gated field emitters used in the experiment have emission half angles that vary from 30° to 45° [16],[17] which is typical of Spindt type [18] gated field emitters, so rather than model each individual emitter, a representative spread of emission was used to approximate an array of emitters. To represent the emission angle, the emitting segment was defined as an arc segment so that electrons are emitted at an angle to the array surface. The resulting electrons then have a transverse velocity component as if emitted from an actual gated emitter. Each of the 24 emitter arcs is identical. The emitter segment voltage is 80 V, and the injected current is 1 µA with an initial kinetic energy of 80 eV, in order to represent the energy of electrons from the actual gated emitter. The current injection is fixed and is not represented by a Fowler-Nordheim [18] current-voltage relation as with the actual emitters. We believe this representation is adequate for the modeling performed here and that using more detailed gated emitter structures would not improve the results. For the energy analysis simulations, 240 rays were used; the surface charge time step was 5 µs, and the hop funnel wall contained 100 elements. The secondary emission parameters were chosen to be $\delta_e = 1.8$, $W_m = 500$ eV, and $W_{avg} = 5$ eV. The anode was set to 750 V.

The vertical electron energy distributions were generated with the hop electrode at 650 V and at 170 V, using the parameters listed above. The 650 V simulation is shown in Fig. 2 and the 170 V case is show in Fig. 8. Both cases are for the steady state regime. For the 650 V case, the hop electrode voltage is high enough to extract all the injected current to obtain unity gain. The vertical energy distribution was calculated from the steady state portion of the simulation, and the result is shown in Fig. 9(a). For the 170 V case, Fig. 8 shows that unity gain is not achieved, and most electrons are simply turned back to the emitter/gate by the large negative surface charge which builds up on the hop funnel wall. The minority of charge rays that do get collected on the anode, however, are used to calculate the resulting vertical energy distribution, as shown in Fig. 9(b).

Hop funnel I-V curves were generated from the simulation for different values of the secondary emission parameters. The current was determined by taking the anode current in the steady state regime at different hop electrode potentials. There are two simulation cases shown in Fig. 10 with one at $\delta_e = 1.75$ and the other at $\delta_e = 2.0$. Both have $W_m = 500$ eV, and $W_{avg} = 5$ eV. As seen from these curves, a decreasing $\delta_e$ results in a shallower slope to the I-V curve. A larger $\delta_e$ will generate a much steeper slope. The same effect can be observed by changing $W_m$. A larger value results in a shallower slope to the knee.

© 2011 IEEE. Personal use of this material is permitted. Permission from IEEE must be obtained for all other uses, in any current or future media, including reprinting/republishing this material for advertising or promotional purposes, creating new collective works, for resale or redistribution to servers or lists, or reuse of any copyrighted component of this work in other works. DOI: 10.1109/TPS.2010.2087775

It should be noted that the values of the secondary emission parameters used here may not represent the actual values of the material (LTCC). This part of the simulation study will be addressed in future work. However, these two simulations give the expected I-V characteristics with the current increasing to unity gain. Also graphed in the figure are the experimental results which are discussed below.

## III. Experimental Results

The hop funnels used in these experiments were fabricated using Dupont 951 Green Tape™ LTCC [12]. The LTCC comes in unfired sheets of varying thickness. These sheets can be pressed together to form thicker layers as desired. The material can be milled to form slits or holes. For this experiment, a 90º bit was used to mill multiple funnels into a single LTCC structure. After milling the LTCC was fired at 700º C to burn out the binder. A thick film silver paste was printed on top of the hop funnel plate to form the hop electrode. Field emission cathodes were then aligned and attached to the hop funnel using a carbon tape. The tape is 0.1 mm thick, so there is a gap from the emitter to the bottom of the hop funnel as shown in Fig. 1.

The emitters used in the hop structure were fabricated by Motorola [19] as part of their FED program and consist of standard Spindt type gate field emitters made from molybdenum with gate diameters of ~ 1 µm. These vertical cone type emitters with surrounding gates are in arrays of 126 emitters per cell or pixel. For our experiments there were 9 pixels per hop funnel opening. These particular emitters had large emitter to gate leakage current, so it was not possible to control the emission current very well.

An anode biased at 750 V was place over the hop funnel exit to measure the current. The hop funnel voltage was swept from 0 V to 550 V and back to 0V over a period of about 20 s. The gate voltage was held at 80V relative to the emitters for an emission current of ~1 µA. The measured I-V characteristics for this funnel for five sweeps are shown in Fig. 9. The results are somewhat noisy, so the experimental error of the I-V curve is high. The current has been normalized for the maximum value for each voltage sweep. The results show a knee and a transition from low current to unity gain over a voltage range of roughly 150 V with a starting value of around 200 V. In some cases the measured current does not go to zero when the hop voltage goes to zero. This result is believed to be related to charging, possibly on the bottom of the hop funnel surface. These results are typical of hop funnel I-V curves [4],[8].

A three electrode energy analyzer was placed directly over the hop funnel to serve as the anode and to measure the vertical electron kinetic energy distribution. This experimental setup is shown in Fig. 11. In this case the energy analyzer collector (anode) was biased 7 V (to suppress secondary emissions off of the anode) positive with respect to ground by a battery. The discriminator grid for the analyzer could be swept from 0 to -1000 V, and the front grid of the analyzer was held at ground as shown in Fig. 11. The field emitter array and hop funnel structures were then floated to -750 V relative to ground. This approach eliminated the need for floating the energy analyzer more positive than the hop funnel. The hop electrode and field emitter gate were then biased positive with respect to the floating voltage of the emitters.

The procedure for measuring the vertical cumulative energy distribution was much the same as the I-V measurement, except the discriminator electrode of the energy analyzer (Fig. 11) was swept from 0 V to -750 V and then back to 0 V while the hop voltage was held constant. Because the emission current was noisy, seven sweeps were done in this manner, and the seven sweeps were averaged. The results are shown in Fig. 12 for the two cases corresponding to the hop electrode biased at relative values of 650 V and 170 V with respect to the cathode (emitter). Also, a monotonic piece-wise linear least-squares curve was fit to the measured vertical cumulative energy distribution, as shown in Fig. 12. The fitting algorithm incorporates a smoothing form factor to help smooth the curve so that the derivative of the cumulative distribution results in the smooth normalized energy distribution of Fig. 9.

## IV. Comparison with Simulation

The comparison of the I-V experimental results with the simulation is quite good over the range of $\delta_e$. These results should not be used to infer that the values of $\delta_e$ and $W_m$ are correct. Nevertheless, the simulation appears to capture the I-V curve shape quite well. The two values of $\delta_e$ bracket the experimental results, and the simulation provides both the correct starting point of the transition at 200 V as well as the slope, within the experimental error. No other adjustments to the simulation are used to shift these values other than the selection of the secondary parameters, $\delta_e$ and $W_m$.

The vertical electron energy distributions in Fig. 9 show two types of electrons: primary and secondary. An electron born at the emitter (-750 V) without any intermediate collisions will have a total energy of 750 eV when it reaches the anode. However, the vertical energy component will be just less than 750 eV due to the angular emission distribution of the emitter. Electrons which hop along the funnel wall before exiting will have lower energies. Fig. 9(a) shows that the electron energy distribution ranges between 100 eV and 750 eV. The lowest energy electrons are a result of those secondary electrons which are born at the highest points in the hop funnel structure, near the exit region where the potential contours are nearly equal to the hop electrode potential of -100 V; these electrons will achieve a vertical energy < 100 eV when they are collected at the anode. Thus, Fig. 9(a) shows that the majority of electrons that exit the hop funnel are secondary electrons produced from the hopping mechanism along the wall, and these electrons are represented by the large low energy peak near 100 eV. Hence, in the unity gain regime, the bulk of the current exiting the hop funnel comes from the hopping process (secondary electrons). Furthermore, the second largest peak occurs at the highest energies near 750 eV, which corresponds to the primary electrons that exit the funnel without striking the sides. Similarly, Fig. 9(b) shows that the energy distribution ranges between 580 eV and 750 eV, as expected from the potential of the hop electrode for part (b) at -580 V and the potential of the cathode at -750V. In this case, the hop electrode voltage is not high enough to sustain the secondary electron hopping transport along the wall, so the

© 2011 IEEE. Personal use of this material is permitted. Permission from IEEE must be obtained for all other uses, in any current or future media, including reprinting/republishing this material for advertising or promotional purposes, creating new collective works, for resale or redistribution to servers or lists, or reuse of any copyrighted component of this work in other works. DOI: 10.1109/TPS.2010.2087775

majority of electrons that make it to the anode are primary electrons corresponding to the highest energy peak near 750 eV, and the secondary electrons that exit the hop funnel are smaller in number and correspond to the smaller peak near 580 eV. The simulation provides a good fit to the experimental data given the finite number of rays used.

The differences between the simulation results of the energy distribution and the results from the measurements are due to the level of noise (25%) in the field emission current, the error in the geometrical representation of the hop funnel used in the simulation, and the uncertainty in the actual values of the secondary emission parameters of LTCC. The geometrical error was estimated to be 8%, and most of this uncertainty is in the representation of the exit region where there is a slight neck thickness that varies across different hop funnels on the same LTCC structure.

## V. Conclusion

The particle trajectory Lorentz 2E was used to model an electron hop funnel. The model includes the build up of surface charge on a dielectric wall and the emission of secondary electrons from the wall. A test case was used to form a basis for stability of the simulation for a hop funnel device with respect to the simulation parameters. Then, experimental measurements of the I-V characteristics and the energy distribution of an LTCC hop funnel device were performed and used as the main diagnostics to compare against the results of the particle trajectory code. The secondary emission parameters for LTCC are unknown, but values were obtained indirectly through comparisons with the experimental results. These parameters, however, can not be uniquely determined from the comparisons described above; rather, there is a continuum of values that can be chosen which closely reproduces the results from the experiment. The result of this comparison indicates that the Lorentz simulation can be used to model electron hopping structures. Future work will investigate the variation of the hop funnel results with secondary parameters as well as the temporal build up of the surface charge on the hop funnel wall.

## Acknowledgments

The authors would like to thank Prof. Don Plumlee, Sonya Shawver, Brandon Wells, Tyler Rowe, and Geoff Groff at Boise State University for their assistance on this project. We would also like to thank Dr. Babu Chalamala for the field emitters.

## References

[1] D. Cathey, "Field emission displays," *Proc. Int. Symp. VLSI Technology, Systems, and Applications*, pp. 131-136, 1995.

[2] T. Utsumi, "Vacuum micro-electronics for future display technology," *Journal of SID*, vol. 1/3, pp. 313-317, 1993.

[3] D.R. Whaley, B.M. Gannon, C.R. Smith, C.M. Armstrong, C.A. Spindt, "Application of field emitter arrays to microwave power amplifiers," *IEEE Trans. On Plasma Science*, vol. 28, pp. 727-747, June, 2000.

[4] BHW Hendriks, GGP van Gorkom, N Lambert and ST de Zwart, "Modes in electron-hopping transport over insulators sustained by secondary electron emission," *J. Phys. D: Appl. Phys.*, vol. 30, pp.1252-1264, 1997.

[5] R.G. Lye and A.J. Dekker, "Theory of secondary emission," *Physical Rev.*, vol. 107, pp. 977-982, 1957.

[6] E.M. Baroody, "A theory of secondary electron emission from metals," *Phys. Rev.*, vol. 78, pp. 780-787, 1950.

[7] K. Kanaya, S. Ono, and F. Ishigaki, "Secondary electron emission from insulators," *J. Phys.D.: Appl. Phys.*, vol. 11, pp.2425-2437, 1978.

[8] R.A. Tuck, W. Taylor, M.S. Waite, H.E. Bishop, R.J. Riggs, and J.J. Browning, "The pFED – A viable route to large field emission displays," 18th Intl. Vacuum Nanoelectronics Conference, Oxford, UK, July, 2005.

[9] L. Min, Z. Xiaobing, L. Wei, Z. Hongping, W. Baoping, "Transverse energy distribution analysis in a filed emission element with an insulator funnel", *Nuc. Instr. and Methods in Phys. Res. B* , vol. 234, pp. 210-218 2005.

[10] W. Lei, X. Zhang, X. Zhou, Z. Zhu, C. Lou, H. Zhao, "Characteristics of a cold cathode electron source combined with a secondary electron emission in a FED," *Appl. Surf. Science*, Vol. 251, pp. 170-176, 2005.

[11] Integrated Engineering Software Inc. OERSTED, Users and Technical Manual, Version 1.0, 46-1313 Border Place, Winnipeg, Manitoba, Canada, R3H 0X4, 1992. Available: http://www.integratedsoft.com

[12] *DuPont 951 Grean Tape™ Product Description*. Available: http://www2.dupont.com/MCM/en_US/assets/downloads/prodinfo/951LTCCGreenTape.pdf

[13] J. Rodney M. Vaughan, "A new formula for secondary emission yield", *IEEE Transactions on Electron Devices*, Vol. 36, pp. 1963-1967, 1989.

[14] J. Rodney M. Vaughan, "Secondary emission formulas", *IEEE Transactions on Electron Devices*, Vol. 40. p. 830, 1993.

[15] *CRC handbook of tables for applied engineering science*, 2nd ed., CRC Press, Boca Raton, FL, May 1973, pp. 316.

[16] C. A. Spindt, C. E. Holland, I. Brodie, J. B. Mooney, and E. R. Westerberg,"Field emitter arrays applied to vacuum fluorescent display," *IEEE Trans. Electron Devices*, vol. 36, pp. 225–228, 1989.

[17] S. Itoh, "Current Status of the Spindt-type Field Emitter", XXIInd Int. Symp. On Disch. And Electr. Ins. In Vacuum, p875, 2006.

[18] C.A.Spindt, I.Brodie, L.Humphrey, and E.R.Westerberg, "Physical properties of thin-film field emission cathodes with molybdenum cones", *J. Appl. Phys*., Vol.47, No.12, pp.5248-5263,1976.

[19] BR Chalamala, Y Wei, BE Gnade, IEEE Spectrum, v35, p42, 1998.

**Charles Lester** (M'08) received a B.S. degree in physics and mathematics from the University of Notre dame, South Bend, Indiana USA in 2002.

He has been a graduate student at Boise State University, Boise, ID, USA in the Electrical and Computer Engineering Department since 2007. His current research interests include Microwave Vacuum Electron Devices.

**Jim Browning** (M'90–SM'08) received a B.S degree and an M.S. in nuclear engineering from the University of Missouri-Rolla, Rolla, MO USA in 1983 and 1985, respectively. He received his PhD from the University of Wisconsin, Madison, WI USA in 1988.

He has been an Associate Professor in the Department of Electrical and Computer Engineering at Boise State University, Boise, ID USA since 2006. Prior to joining BSU, he was a consultant on field emission technology, worked as a Senior Development Engineer at PixTech, Inc and at Micron Technology, Inc. His research interests are in Microwave Vacuum Electron Devices (MVEDs) and plasma propulsion.

**Lael Matthews** received a B.S. degree in control systems engineering from the United States Naval Academy, Annapolis, MD USA in 2000. He received his Masters Degree in Electrical Engineering 2010 and is currently working at Micron Tech. in Boise, ID USA.

© 2011 IEEE. Personal use of this material is permitted. Permission from IEEE must be obtained for all other uses, in any current or future media, including reprinting/republishing this material for advertising or promotional purposes, creating new collective works, for resale or redistribution to servers or lists, or reuse of any copyrighted component of this work in other works. DOI: 10.1109/TPS.2010.2087775

Table I: Simulation runs for different numbers of rays and time step sizes. Each column has the same number of electrons per ray whereas each row has the same number of rays. The column labels are in units of thousands of electrons per ray (ke/ray).

| | **3.1 (ke/ray)** | **31 (ke/ray)** | **310 (ke/ray)** |
|---|---|---|---|
| **$\Delta t_1$ (μs) / $N_1$** | 0.1 / 200 | 1 / 200 | 10 / 200 |
| **$\Delta t_2$ (μs) / $N_2$** | 0.05 / 100 | 0.5 / 100 | 5 / 100 |
| **$\Delta t_3$ (μs) / $N_3$** | 0.025 / 50 | 0.25 / 50 | 2.5 / 50 |

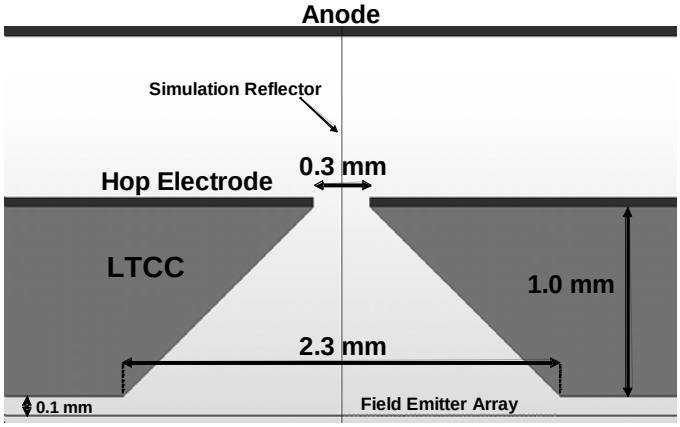


Fig. 1. Simulation geometry setup of the hop funnel showing electrodes and dimensions. The funnel is rotationally symmetric about the center vertical line. The grey region is the LTCC hop funnel, which is placed 0.1 mm above the cathode (FEA).

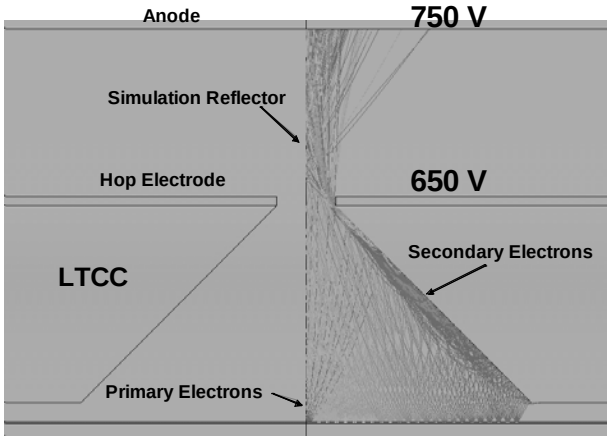


Fig. 2. Simulation showing primary and secondary electron rays with the hop electrode at 650 V. The simulation reflector reflects the incoming charge rays about the line shown. At 650 V, the number of extracted rays approximately equals the number of injected rays for unity gain.

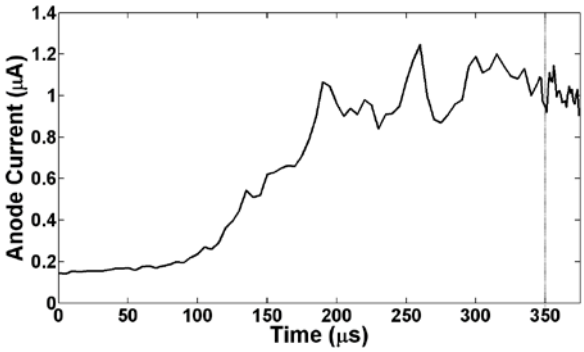


Fig. 3. Simulated anode current vs. time. This is the initial time step sequence that is used for the first two columns of Table 1. The sequence consists of 5 μs time steps for surface charge time step iterations 1 – 69, and then 1 μs time steps for iterations 70 – 99. The vertical line drawn at 350 μs corresponds to the 5 μs to 1 μs change.

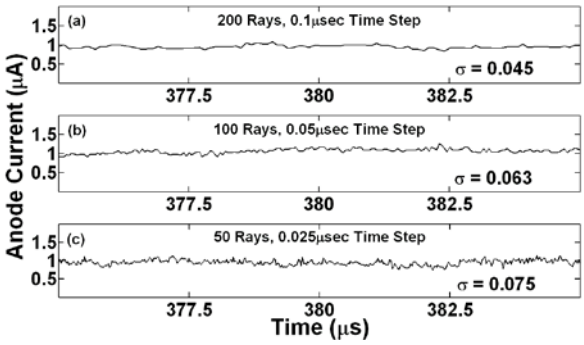


Fig. 4. Steady state current from the simulation after 380 μs for 3121 electrons per injected ray for the cases of (a) 200 injected rays with 0.1 μs time step, (b) 100 rays with 0.05 μs time step, and (c) 50 rays with 0.025 μs time step.

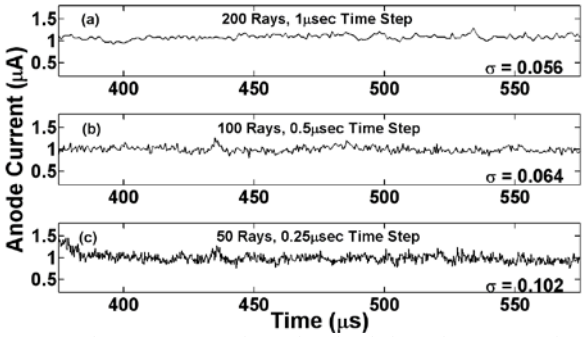


Fig. 5. Steady state current from the simulation after 380 μs for 31210 electrons per injected ray for the cases of (a) 200 injected rays with 1.0 μs time step, (b) 100 rays with 0.5 μs time step, and (c) 50 rays with 0.25 μs time step.

© 2011 IEEE. Personal use of this material is permitted. Permission from IEEE must be obtained for all other uses, in any current or future media, including reprinting/republishing this material for advertising or promotional purposes, creating new collective works, for resale or redistribution to servers or lists, or reuse of any copyrighted component of this work in other works. DOI: 10.1109/TPS.2010.2087775

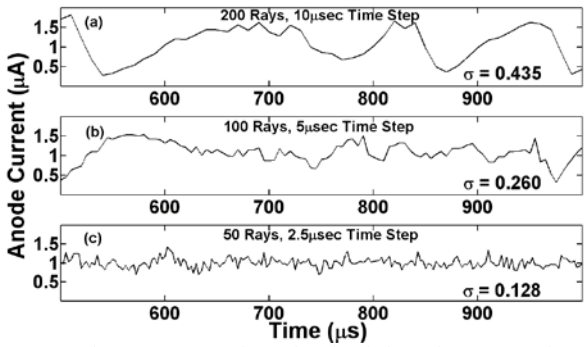


Fig. 6. Steady state current from the simulation after 380 μs for 312100 electrons per injected ray for the cases of (a) 200 injected rays with 10 μs time step, (b) 100 rays with 5 μs time step, and (c) 50 rays with 2.5 μs time step.

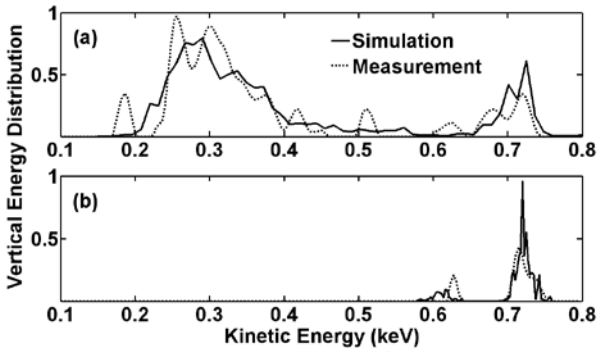


Fig. 9. Normalized vertical energy distribution from the experiment and from the simulation for (a) with the hop electrode at 650 V and (b) with the hop electrode at 170 V. The energy distribution shifts from mostly secondary electrons in (a) to mostly primary electrons in (b).

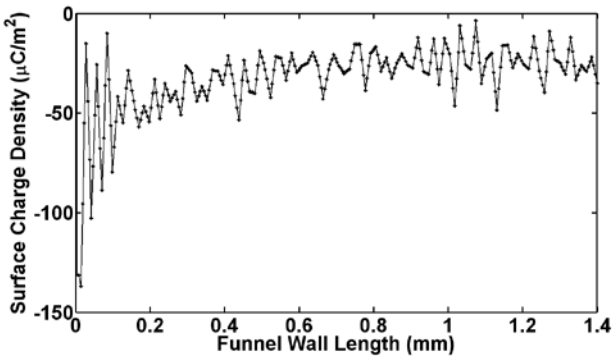


Fig. 7. Hop funnel surface charge density, for the case of Fig. 5(a), as a function of length along the hop funnel wall, starting from the hop funnel exit at 0 mm to the hop funnel entrance at 1.414 mm. The plotted points correspond to each of the 100 surface elements that the hop funnel wall is divided into.

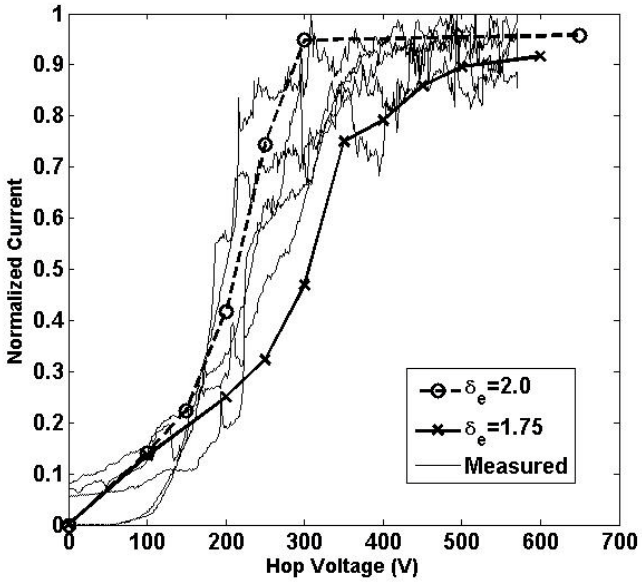


Fig. 10. The I-V characteristics of the hop funnel for both experiment and simulation. Current is normalized to the maximum value for the experiment.

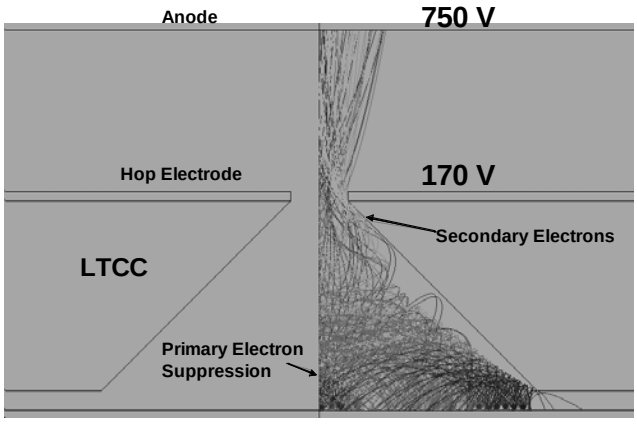


Fig. 8. Simulation showing primary and secondary electron rays with the hop electrode at 170 V. Rays are turned back by the negative surface charge distribution on the hop funnel wall and are collected on the gate/emitter structure.

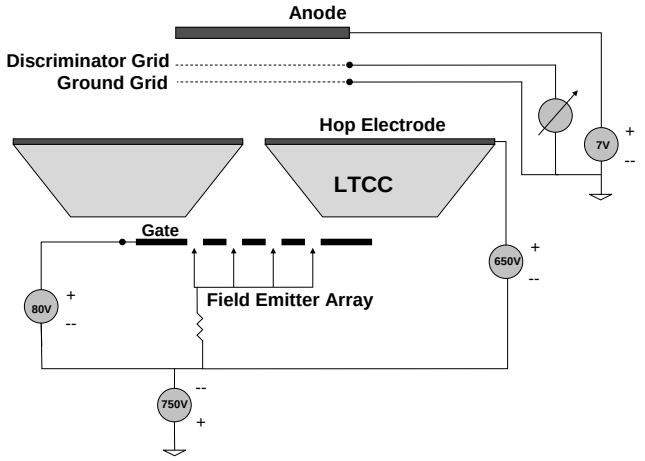


Fig. 11. Experimental test setup for energy analyzer measurements with the cathode biased negative with respect to ground.

© 2011 IEEE. Personal use of this material is permitted. Permission from IEEE must be obtained for all other uses, in any current or future media, including reprinting/republishing this material for advertising or promotional purposes, creating new collective works, for resale or redistribution to servers or lists, or reuse of any copyrighted component of this work in other works. DOI: 10.1109/TPS.2010.2087775

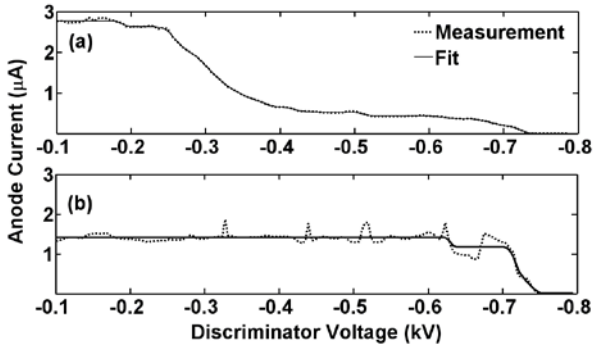


Fig. 12. Measured current from the energy analyzer vs discriminator voltage for the hop funnel electron beam with a monotonic piece-wise linear least-squares curve fit, with the hop electrode at (a) 650 V and at (b) 170 V. In each case, the fitting algorithm incorporates a smoothing form factor to help smooth the monotonic fit curve.